Raman investigation of anharmonicity and disorder-induced effects in $Zn_{1-x}Be_xSe$ epifilms

L. Y. Lin, C. W. Chang, W. H. Chen, and Y. F. Chen
Department of Physics, National Taiwan University, Taipei, Taiwan, 106 Republic of China

S. P. Guo and M. C. Tamargo
Center for Advanced Technology on Ultrafast Photonic Materials and Applications, Center for Analysis of Structures and Interfaces (CASI), Department of Chemistry, City College-CUNY, New York, New York 10031, USA

(Received 25 June 2003; published 17 February 2004)

Raman scattering of $Zn_{1-x}Be_xSe$ epifilms grown by molecular beam epitaxy on GaAs (001) substrates has been investigated. The effect of compositional disorder was obtained by analyzing the broadening and asymmetry of the first-order LO mode. It is found that the Raman line shapes for the ZnSe-like LO mode in $Zn_{1-x}Be_xSe$ alloys can be well described by the spatial correlation model. We have also analyzed comparatively the anharmonic effects due to temperature and compositional fluctuations in ZnSe and ZnBeSe systems, using temperature-dependent Raman-scattering measurements. It is found that the anharmonicity is higher for ZnBeSe alloys than ZnSe and it increases with compositional disorder. Therefore, both temperature- and compositional-fluctuation-induced anharmonicities can introduce changes in the linewidth, line center position, and anharmonic decay time of the first-order optical phonons in $Zn_{1-x}Be_xSe$ alloys.

DOI: 10.1103/PhysRevB.69.075204 PACS number(s): 78.30.Fs, 63.20.Ry

I. INTRODUCTION

A new interest in ZnSe-based systems has arisen in view of recent calculations[1] which predicted a large amount of covalent bonding for Be chalcogenides. A concomitant increase in the lattice strength is expected to have a significant influence on the defect generation and propagation.[2] It is therefore that ZnBeSe alloys are actually very promising for both academic interest and industrial applications. Some research efforts have been carried out in order to elucidate the intrinsic properties of ZnBeSe alloys.[3–9] Concerning the vibrational properties, the zone-center $(q\sim 0)$ longitudinal-optical (LO) and transverse-optical (TO) phonons of BeSe and $Zn_{1-x}Be_xSe$ alloys were recently identified by using infrared and Raman spectroscopies.[10,11] Since Raman scattering can yield important information about a solid on a scale of the order of a few lattice constants, it can be used to study the microscopic nature of structural or topological disorder. Although there have been a few Raman studies of $Zn_{1-x}Be_xSe$ alloys, only little attention was awarded to the relation between the alloy disorder and the line shape (i.e., linewidth and asymmetry) of allowed modes. In this paper, we will provide a detailed investigation on the influence of the first-order Raman spectra caused by alloy potential fluctuations (APF's) in ZnBeSe alloys.

In ternary semiconductor alloys, the Raman spectra show changes of various phonon modes with compositional disorder, including a shift in phonon frequency and changes of the linewidth, asymmetry, and emergence of disorder-activated modes. The broadening in linewidth and asymmetry can be investigated in terms of the spatial correlation (SC) model[12,13] based on the finite correlation length of a propagating phonon due to the APF's. In addition, a change in crystal temperature also introduces a softening of phonon frequencies, a broadening of line shapes, and a decrease in intensity. Balkanski, Wallis, and Haro[14] and some other authors[15,16] have found changes of the linewidth and line center for the optical modes at the center of the Brillouin zone in crystalline Si with temperature due to anharmonic effects in the vibrational potential energy. Later, a huge body of literature has described the temperature behavior of the Raman spectra for materials such as Si from low temperature to melting.[17,18] But less information exists for the anharmonic effect in ternary alloys. Beserman *et al.*[19] demonstrated that the anharmonicity varies with the composition in $In_{1-x}Ga_xP$. Jusserand and Sapriel[20] have investigated a GaAs-like LO phonon in $Al_xGa_{1-x}As$ epitaxial layers with $x=0.27$ and observed that anharmonicity is not affected by substitutional disorder. Ramkumar *et al.*, who observed the anharmonicity in $GaAs_{1-x}P_x$ and $In_xGa_{1-x}As$,[21] and Minén-dez *et al.*, who studied on $Al_xGa_{1-x}As$,[22] have found that in ternary systems the anharmonic effect increases with an increase in substitutional disorder. Although the above studies have been devoted to the anharmonicity as a function of compositional variation in III-V ternary crystals, to our knowledge no detailed work has been reported on the anharmonicity in II-VI ternary alloys. For the purpose we will investigate anharmonic effects due to the change of temperature in ZnSe and due to both of the changes of temperature and compositional disorder in $Zn_{1-x}Be_xSe$. It is then possible to make a comparative study of anharmonic effects in binary and ternary II-VI semiconductor alloys. In addition, the effect of alloy potential fluctuations on the first-order Raman spectra of $Zn_{1-x}Be_xSe$ epifilms will also be discussed in detail using the SC model.

II. EXPERIMENTAL PROCEDURE

High-crystalline-quality $Zn_{1-x}Be_xSe$ ($x=0$, 3.14%, 5.43%, 9.13%) epilayers (1 μm thick) were grown on GaAs (001) substrates by molecular beam epitaxy (MBE). A ZnSe cap layer ($\sim$5 nm thick) was deposited on the epilayer to protect against post-growth oxidation. A novel method of Be-Zn coirradiation, before growth of a 10-nm ZnSe buffer

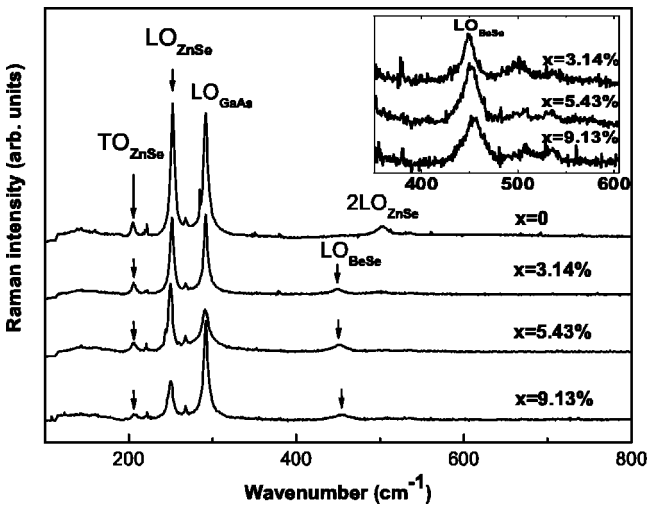

FIG. 1. Raman spectra of $Zn_{1-x}Be_xSe$/GaAs in backscattering geometry along the growth axis at room temperature. The inset clearly indicates the BeSe-like longitudinal optical mode in ZnBeSe alloys.

layer, was used in order to avoid the formation of stacking faults at the III-V/II-VI interface. For a more detailed description of the growth procedure and growth parameter see Guo *et al.*[23]

The Raman spectra were recorded in a backscattering configuration using a JOBIN YVON-SPEX (model T 64000) micro-Raman spectrometer with a charge-coupled detector (CCD) and confocal optics at different temperatures. The sample was held in an open cycle helium cryostat, and the temperature could be controlled from 6 to 306 K. The temperature accuracy is better than ± 1 K. The 488-nm line of an Ar-ion laser was used to excite the sample, and the laser power supplied through the objective lens was estimated to be less than 120 mW incident on the sample into a focused spot ~ 1 μm. To ensure a signal-to-noise ratio greater than 100:1, small slits and long integration times were used. The spectral resolution was less than 0.5 cm^{-1}.

III. RESULTS AND DISCUSSION

Representative spectra obtained in backscattering along the growth axis at room temperature are shown in Fig. 1. We first comment on the signal corresponding to the substrate side. The longitudinal optical mode from GaAs is evidenced at 292 cm^{-1}, but a rather weak line corresponding to the forbidden transverse optical mode is also observed at 268 cm^{-1}. The observation of this symmetry-forbidden TO signal in backscattering geometry from the (100) GaAs substrate can arise from a variety of sources including elastic scattering by ionized dopant impurities, deviation from the strict backscattering geometry, misorientation of the GaAs film due to contamination, internal strain, etc. According to the fact that the ratio of the Raman intensity between the GaAs-TO mode and GaAs-LO mode is less than 1%, the deviation from strict backscattering geometry should be very small, which should not have any significant influence on the properties discussed below.

We now turn to the epilayer-related signals. The structures of the first-order phonons at 205 and 257 cm^{-1} from ZnSe correspond to the weak forbidden TO and allowed LO modes, respectively. The two-phonon LO mode in the Raman spectrum of ZnSe appears due to scattering involving two successive first-order processes. The spectra of the $Zn_{1-x}Be_xSe$ alloys show a typical two-mode-type behavior, as expected from the modified-random-element-isodisplacement (MREI) model[24] since the mass of substituting element beryllium is smaller than the reduced mass of ZnSe. The peaks labeled as LO_{ZnSe} and LO_{BeSe} are, respectively, identified as ZnSe-like and BeSe-like LO phonons. However, we notice that the strengths of LO_{ZnSe} weaken as the concentration of Be increases, but on the other hand the strengths of LO_{BeSe} enhance relatively. The BeSe-type LO mode shows an increase of frequency with decreasing density of the ZnSe content, as indicated in the inset of Fig. 1. At low content of Be, because of the lattice mismatch between ZnSe and BeSe, Be-Se bonds undergo a tensile strain owing to the ZnSe-like matrix, which reduces the effective force constant. This gives rise to local BeSe-like modes emerging between 448 and 453 cm^{-1}, and showing a redshift frequency with decreasing Be concentration.

Figure 1 shows that the Raman full width of half maximum (FWHM) for the ZnSe-like LO phonon in $Zn_{1-x}Be_xSe$ epifilms increases with increasing Be composition. For the pure ZnSe film, the Raman line shape displays a symmetric Lorentzian profile. The asymmetric ratio $[\Gamma_l/\Gamma_h$, where Γ_l (Γ_h) represents the low-energy (high-energy) half width of half maximum in the phonon signal] of the LO_{ZnSe} peak in general increases with the Be content. On the other hand, as the weak ZnSe-like TO mode is observed in Fig. 1, the intensity ratio of the forbidden TO to the allowed LO phonons for the ZnSe-like modes in $Zn_{1-x}Be_xSe$ alloys increases with increasing x. The increases of FWHM, Γ_l/Γ_h, and I_{TO}/I_{LO} are clearly driven by the addition of Be atoms. Atom substitution induces not only topological disorder, but often also structural disorder. For allowed phonons these disorders result basically in the breaking of the translational symmetry, leading to the contribution of $q \neq 0$ phonons to Raman line shape, corresponding to so-called finite-size effects. This greatly drives the line shape asymmetry and the progressive activation of zone-center mode which is theoretically forbidden, as detailed above.

Here we discuss the effects of disorders in $Zn_{1-x}Be_xSe$ alloys using the SC model.[13,25] In an ideal crystal, the region over which the spatial correlation function of the phonon extends is infinite. As the crystal is alloying, the spatial correlation length of the phonon becomes finite owing to the potential fluctuations of the alloy disorder, which gives rise to a relaxation of the $q=0$ selection rule in Raman scattering.[26] The finite phonon mode will lead to the broadening and asymmetry of the Raman line shape. With the SC model, we can evaluate the asymmetric broadening of Raman scattering by the theoretical calculation. The assumption of a Gaussian attenuation factor $\exp(-2r^2/L^2)$, where L is the diameter of the correlation region, has been successfully used to account for q-vector relaxation related to finite-size effects[25] and structural disorder (ion-damaged materials).[12]

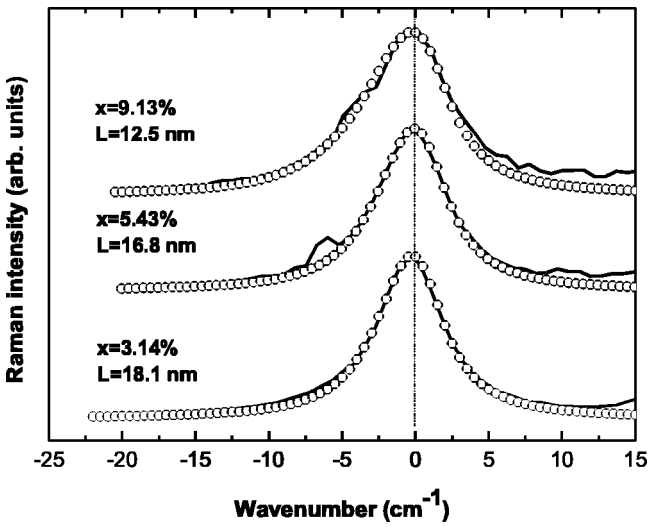

FIG. 2. Experimental and calculated line shapes of the ZnSe-like longitudinal optical mode for $Zn_{1-x}Be_xSe$ with $x=3.14\%$, 5.43%, and 9.13%. These are artificially centered at 0 cm^{-1} for a better comparison of the line shapes. The lines correspond to experimental data. The open dots show the theoretical fits obtained by using the spatial correlation model. The corresponding correlation lengths L are reported in front of each spectrum.

Assuming that there is a spherical region associated with the finite size of the correlation regions in the alloys, the Raman intensity $I(\omega)$ at a frequency ω can be written as

$$I(\omega)\sim\int_0^1 \exp\left(\frac{-q^2L^2}{4}\right)\frac{d^3q}{[\omega-\omega(q)]^2+\left(\frac{\Gamma_0}{2}\right)^2}, \qquad (1)$$

where q is expressed in units of $2\pi/a$, a is the lattice constant, and Γ_0 is the linewidth of the ZnSe LO phonon in the pure ZnSe epilayer. We take the dispersion $\omega(q)$ of the LO phonon based on a one-dimensional chain model:

$$\omega^2(q)=A+\{A^2-B[1-\cos(\pi q)]\}^{1/2}, \qquad (2)$$

where $A=3.2\times10^4$ cm^{-1} and $B=4.5\times10^8$ cm^{-1} for ZnSe.[27] By setting the correlation length L as an adjustable parameter, one can try to describe the experimental data by the SC model. The best fits are reported in Fig. 2. The L values corresponding to $x\sim3.14\%$, 5.43%, and 9.13% are 18.1, 16.8, and 12.5 nm, respectively. In the two-mode behavior alloys such as $Zn_{1-x}Be_xSe$, we can consider that the ZnSe- and BeSe-like phonon modes are localized in the ZnSe and BeSe regions, respectively. The ZnSe-like phonon correlation length L can be physically interpreted as the average size of the localized region of ZnSe-like phonons. The value of L decreases with increasing Be composition; the phonon extended region becomes very small. This is caused by the compositional disorder in alloys. Therefore, the L value is a very appropriate parameter accounting for the disorder of $Zn_{1-x}Be_xSe$ alloys.

The first-order Raman spectra of $Zn_{1-x}Be_xSe$ alloys were investigated from 6 to 306 K. The LO mode for ZnSe and the LO_{ZnSe} mode for the representative alloy ($Zn_{1-x}Be_xSe$, $x=9.13\%$) at variable temperatures are shown in Fig. 3. It points out that as the temperature increases the frequency for the LO mode in ZnSe and the LO_{ZnSe} mode in ZnBeSe alloy decreases, the intensity decreases, and the Raman linewidth increases. In order to understand this behavior, we will adapt the theoretical work developed by Balkanski, Wallis, and Haro.[14] They have explained the variation by the anharmonicity in vibrational potential energy, which leads to the decay of an optical phonon into two, three, or more acoustic phonons, giving rise to cubic and quartic or higher-order anharmonicities. Taking into account the contributions from cubic and quartic anharmonic terms, the anharmonicity produces a shift Δ in the line center and a finite linewidth Γ related to the vibration damping:

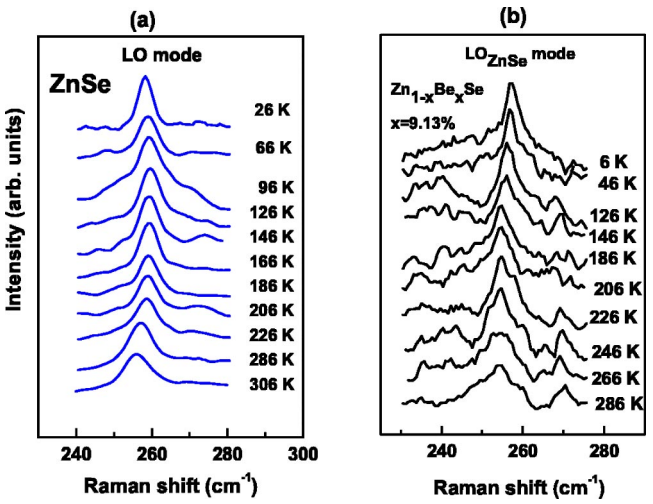

FIG. 3. First-order Raman spectra recorded at variable temperatures for (a) the LO mode in ZnSe and (b) the ZnSe-like LO mode in $Zn_{1-x}Be_xSe$ ($x=9.13\%$) alloy.

$$\omega=\omega_0+\Delta(T) \qquad (3)$$

is the frequency of the phonon in the anharmonic lattice, where ω_0 is the intrinsic frequency of the optical phonon at the Brillouin-zone center in harmonic approximation. The effective half-width Γ can be decomposed into two contributions: a damping Γ_a due to the anharmonicity and a damping Γ_0 independent of T due to other attenuation processes (such as elastic scattering of phonon by defects or disorder in the alloys) (Ref. 28):

$$\Gamma=\Gamma_0+\Gamma_a. \qquad (4)$$

Let us consider Δ and Γ_a due to anharmonicity. One can write

$$\Delta(T)=C\left[1+\frac{2}{e^x-1}\right]+D\left[1+\frac{3}{e^y-1}+\frac{3}{(e^y-1)^2}\right] \qquad (5)$$

and

$$\Gamma_a=A\left[1+\frac{2}{e^x-1}\right]+B\left[1+\frac{3}{e^y-1}+\frac{3}{(e^y-1)^2}\right], \qquad (6)$$

where $y=\hbar\omega_0/3k_BT$ and $x=\hbar\omega_0/2k_BT$. The constants A and C are related to three-phonon process (cubic anharmonicity),

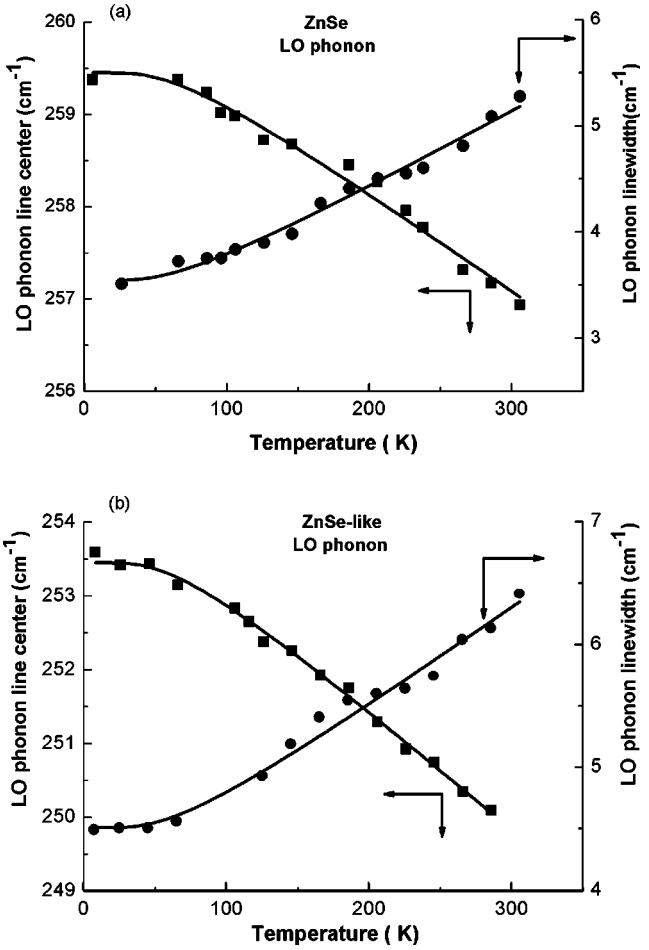

FIG. 4. Temperature dependence of the line center and linewidth for (a) the LO phonon in ZnSe and (b) the ZnSe-like LO phonon in $Zn_{1-x}Be_xSe$ ($x=9.13\%$) alloy.

while the constants B and D are related to four-phonon process (quartic anharmonicity). As temperatures much below the Debye temperature, the contribution from higher-order anharmonic terms (quartic) is negligible. In this case, the important contribution is from the cubic anharmonic term, so that

$$\omega(T)=\omega_0+C\left[1+\frac{2}{e^x-1}\right] \tag{7}$$

and

$$\Gamma(T)=\Gamma_0+A\left[1+\frac{2}{e^x-1}\right]. \tag{8}$$

Hence Eqs. (7) and (8) can be used to describe the temperature dependence of the line center and linewidth of the first-order LO mode at the Brillouin-zone center. The average experimental values of the linewidth and line center for the first-order LO mode in Raman spectra of ZnSe at each temperature are plotted in Fig. 4(a). Equations (7) and (8) are used to fit the experimental data by suitably choosing the constants ω_0, Γ_0, A, and C, which are given in Table I. Figure 4(a) shows that the agreement between the calculated

TABLE I. Best-fit values of the anharmonic constants for the LO mode in ZnSe and the ZnSe-like LO mode in $Zn_{1-x}Be_xSe$ alloys.

Sample	A (cm^{-1})	C (cm^{-1})	ω_0 (cm^{-1})	Γ_0 (cm^{-1})
ZnSe	0.672	−1.028	260.479	2.884
$x=3.14\%$	0.723	−1.430	258.846	3.097
$x=5.43\%$	0.746	−1.471	257.599	3.453
$x=9.13\%$	0.757	−1.529	254.977	3.752

curve, given by the solid line, and the experimental points is quite good. For ZnBeSe alloys, due to the presence of a broad asymmetric ZnSe-like LO mode, we extract the peak frequency and linewidth of the highest-energy phonon ($q\sim 0$ phonon) by fitting only the high-energy part of the Raman band with a Lorentzian.[29] The average values of the line center and linewidth of the highest-energy ZnSe-like Raman band for $Zn_{1-x}Be_xSe$ ($x=9.13\%$) at different temperatures are plotted by small points, and the solid lines show the best fits to the experimental results in Fig. 4(b). The figure of data is a good representation of other ZnBeSe alloys as well. The best values of these constants for $Zn_{1-x}Be_xSe$ alloys are also listed in Table I. We can see from Table I that the anharmonic constants A and C are numerically greater for ZnBeSe alloys than for ZnSe, which indicates that the degree of anharmonicity experienced by the first-order ZnSe-like LO mode in $Zn_{1-x}Be_xSe$ is greater than that of the LO mode in ZnSe. Figures 5 and 6 show the comparisons in the line center and linewidth between the LO mode for ZnSe and the ZnSe-like LO mode for $Zn_{1-x}Be_xSe$ as a function of temperature, respectively. From the figures, we can see that the faster temperature-dependent changes (slightly greater slopes) in the line center and linewidth for $Zn_{1-x}Be_xSe$ than for ZnSe. This behavior can be easily understood as follows. In ZnSe, the anharmonicity depends only upon the temperature and increases with increasing temperature. In $Zn_{1-x}Be_xSe$ alloys, there are two components of anharmonicity, one correspond-

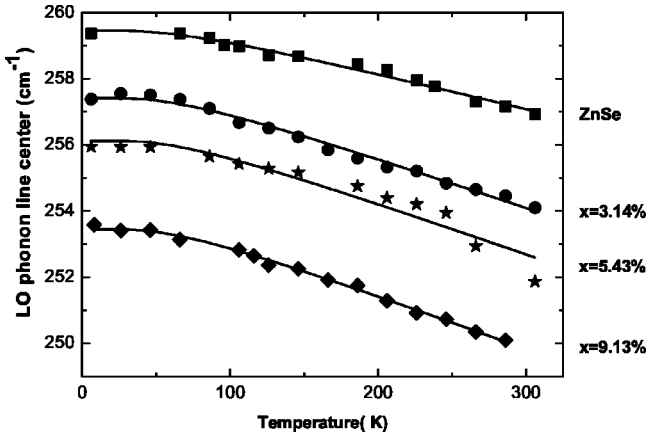

FIG. 5. Comparison of temperature dependence of the line center for the LO mode in ZnSe and the ZnSe-like LO phonon in $Zn_{1-x}Be_xSe$ alloys. The points correspond to experimental data. The solid lines show the theoretical fits obtained by using Eq. (7).

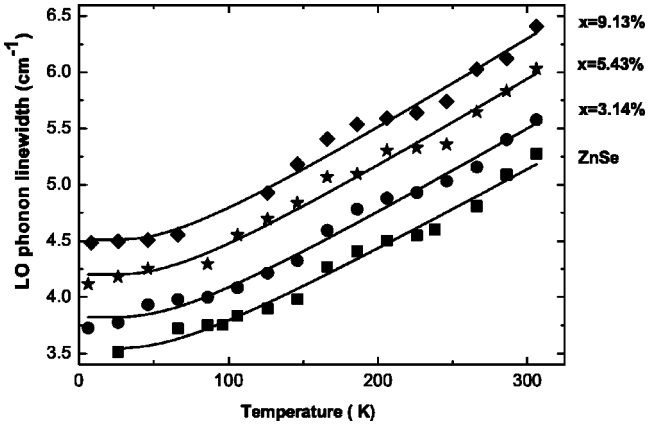

FIG. 6. Comparison of temperature dependence of the linewidth for the LO mode in ZnSe and the ZnSe-like LO phonon in $Zn_{1-x}Be_xSe$ alloys. The points correspond to experimental data. The solid lines show the theoretical fits obtained by using Eq. (8).

ing to temperature and the other to compositional disorder. The compositional-fluctuation-induced anharmonicity is also sensitive to temperature. As the temperature increases, there are larger numbers of phonons produced, resulting in an increase for the probability of inelastic (anharmonic) scattering between phonons and the substitutive atoms. If the number of the substitutive atoms increases, the probability of inelastic decay of phonons becomes larger. Thus increasing temperature makes the compositional-disorder-induced anharmonicity more obvious. At low temperature, we can qualitatively separate out the two components of the anharmonicity by comparing the anharmonicity-induced effects in ZnSe and ZnBeSe systems, because at low temperatures anharmonicity is mainly due to compositional disorder. Figure 7 shows the effect of compositional-disorder-induced anharmonicity on the line center and linewidth of the LO mode in ZnSe and the ZnSe-like LO mode $Zn_{1-x}Be_xSe$ alloys at 6 K. We observe that a large redshift in phonon frequency and an increase in width at low temperature are driven by an increase of compositional disorder. This observation indicates that in ZnBeSe systems, the compositional-disorder-induced

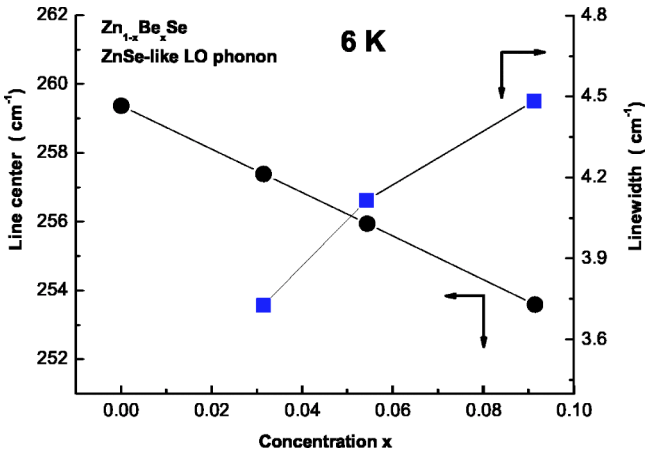

FIG. 7. Concentration dependence of the line center and linewidth for the ZnSe-like LO phonon in $Zn_{1-x}Be_xSe$ alloys at 6 K.

TABLE II. Anharmonic decay time of the first-order LO mode in ZnSe and the ZnSe-like LO mode in $Zn_{1-x}Be_xSe$ alloys at various temperatures.

Temperature (K)	Lifetime (ps)			
	$x=0$	$x=3.14\%$	$x=5.43\%$	$x=9.13\%$
6		8.44	8.02	7.26
26	8.46	7.84	7.29	7.12
146	4.83	4.32	3.83	3.71
226	3.18	2.89	2.83	2.81
266	2.75	2.57	2.41	2.33
306	2.21	2.14	2.05	1.99

anharmonicity causes a redshift in the phonon frequency and a change in the linewidth. Therefore, the substitutive atoms like Be in the ZnSe matrix act as scattering centers for an incoming phonon, and each scattering center promotes anharmonic decay, leading to a redshift frequency and a broadening of width for the ZnSe-like LO phonon.

Finally, the analysis of the linewidth broadening in the Raman measurements can be used as an indirect measurement for estimating the lifetime of the first-order optical phonon at the Brillouin-zone center. There are two processes which induce lifetime of optical phonons: (1) anharmonic (inelastic) decay into lower-energy phonons (decay time $\tau_{\text{anharmonic}}$) and (2) elastic scattering due to disorder or defects (scattering time τ_{elastic}).[30] We therefore write the linewidth of the LO mode as

$$\Gamma(T)=\Gamma_0+A\left[1+\frac{2}{e^x-1}\right]=\frac{1}{2\pi c\,\tau_{\text{elastic}}}+\frac{1}{2\pi c\,\tau_{\text{anharmonic}}}, \tag{9}$$

where $1/2\pi c\,\tau_{\text{elastic}}$ $(=\Gamma_0)$ arises from elastic scattering, $1/2\pi c\,\tau_{\text{anharmonic}}$ $(=A[1+2/(e^x-1)])$ arises from anharmonic decay, and c is the velocity of light. The values of anharmonic decay time $\tau_{\text{anharmonic}}$ for the LO phonon in ZnSe and the ZnSe-like LO phonon in $Zn_{1-x}Be_xSe$ alloys calculated by using Eq. (9) are listed in Table II. Our results show that the anharmonic decay time of first-order LO phonons in ZnSe decreases with increasing temperature and in $Zn_{1-x}Be_xSe$ it decreases with increasing temperature and increasing compositional disorder. Hence compositional disorder can promote the shortening of anharmonic decay time.

IV. CONCLUSION

Raman scattering of $Zn_{1-x}Be_xSe$ epifilms have been performed. We have shown that the increases of the FWHM and asymmetric ratio for the LO mode in $Zn_{1-x}Be_xSe$ can be induced by compositional disorder. The intensity ratio of TO to LO phonons which increases with the concentration of Be can also be interpreted by disorder-induced Raman scattering. The Raman line shapes of the ZnSe-like LO mode in $Zn_{1-x}Be_xSe$ alloys have been analyzed by the spatial correlation model. We have found that the coherence length of the ZnSe-like LO phonon decreases with increasing Be composition due to alloy potential fluctuations.

A comparative study of temperature-dependent Raman scattering from the zone-center LO phonon in ZnSe and ZnBeSe systems shows that the anharmonic constants for ZnBeSe alloys are greater than those for ZnSe and increase with the Be concentration. In ZnSe the anharmonicity increases with increasing temperature, while in ZnBeSe alloys it increases with increasing temperature and composition fluctuations. Both thermal and compositional-disorder-induced anharmonicities introduce a redshift in the phonon frequency, a broadening in the linewidth, and a shortening in anharmonic decay time of the first-order LO phonons.

ACKNOWLEDGMENTS

This work was supported by the National Science Council and Ministry of Education of Republic of China.

[1] C. Vérié, in *Semiconductors Heteroepitaxy*, edited by B. Gil and R. L. Aulombard (World Scientific, Singapore, 1995), p. 73.
[2] F. Vigué, E. Tournié, and J.-P. Faurie, Appl. Phys. Lett. **76**, 242 (2000).
[3] E. Kato, H. Noguchi, M. Nagai, H. Okuyuma, S. Kijima, and A. Ishibashi, Electron. Lett. **34**, 282 (1998).
[4] D. C. Grillo, M. D. Ringle, G. C. Hua, J. Han, and R. L. Gunshor, J. Vac. Sci. Technol. B **13**, 720 (1995).
[5] A. Waag, Th. Litz, F. Fischer, H.-J. Lugauer, T. Baron, K. Schüll, U. Zehnder, T. Gerhard, U. Lunz, M. Keim, G. Reuscher, and G. Landwehr, J. Cryst. Growth **184/185**, 1 (1998).
[6] C. Verie, J. Cryst. Growth **184/185**, 1061 (1998).
[7] S. P. Guo, Y. Luo, W. Lin, O. Maksimov, M. C. Tamargo, I. Kuskovsky, C. Tian, and G. F. Neumark, J. Cryst. Growth **208**, 205 (2000).
[8] C. C. Chu, T. B. Ng, J. Han, G. C. Hua, R. L. Gunshor, E. Ho, E. L. Warlick, L. A. Kolodziejski, and A. V. Nurmikko, Appl. Phys. Lett. **69**, 602 (1996).
[9] F. Fischer, M. Keller, T. Gerhard, T. Behr, T. Litz, H. J. Lugauer, M. Keim, G. Reuscher, T. Baron, A. Waag, and G. Landwehr, J. Appl. Phys. **84**, 1650 (1998).
[10] O. Pagès, M. Ajjoun, J. P. Laurenti, D. Bormann, C. Chauvet, E. Tournié, and J. P. Faurie, Appl. Phys. Lett. **77**, 519 (2000).
[11] A. M. Mintairov, F. C. Peins, S. Lee, U. Bindley, J. K. Furdyna, S. Raymond, J. L. Merz, V. G. Melehin, and K. Sadchikov, Semiconductors **33**, 1021 (1999).
[12] P. M. Amirtharaj, K. K. Tiong, F. H. Pollack, and D. E. Aspnes, Appl. Phys. Lett. **44**, 122 (1984).
[13] P. Parayanthal and F. H. Pollack, Phys. Rev. Lett. **52**, 1822 (1984).
[14] M. Balkanski, R. F. Wallis, and E. Haro, Phys. Rev. B **28**, 1928 (1983).
[15] P. G. Klemens, Phys. Rev. **148**, 845 (1966).
[16] T. R. Hart, R. L. Aggarwal, and B. Lax, Phys. Rev. B **1**, 638 (1970).
[17] J. Menéndez and M. Cardona, Phys. Rev. B **29**, 2051 (1985).
[18] H. Tang and I. P. Herman, Phys. Rev. B **43**, 2299 (1991).
[19] R. Beserman, C. Hirliman, M. Balkanski, and J. Chevallier, Solid State Commun. **20**, 485 (1976).
[20] B. Jusserand and J. Sapriel, Phys. Rev. B **24**, 7194 (1981).
[21] C. Ramkumar, K. P. Jain, and S. C. Abbi, Phys. Rev. B **53**, 13 672 (1996).
[22] J. Menéndez, E. Martín, A. Torres, and J. P. Landesman, Phys. Rev. B **58**, 10 463 (1998).
[23] S. P. Guo, Y. Luo, W. Lin, O. Maksimov, M. C. Tamargo, I. Kuskovsky, C. Tian, and G. F. Neumark, J. Cryst. Growth **208**, 205 (2000).
[24] I. F. Chang and S. S. Mitra, Phys. Rev. **172**, B924 (1968).
[25] H. Richter, Z. P. Wang, and L. Ley, Solid State Commun. **39**, 625 (1981).
[26] Kouji Hayashi, Nobuhiko Sawaki, and Isamu Akasaki, Jpn. J. Appl. Phys., Part 1 **30**, 501 (1991).
[27] D. J. Olego, K. Shahzad, D. A. Cammack, and H. Cornelissen, Phys. Rev. B **38**, 5554 (1988).
[28] D. Mihailovic, K. F. McCarty, and D. S. Ginley, Phys. Rev. B **47**, 8910 (1993).
[29] K. Sinha, A. Mascarenhas, G. S. Horner, K. A. Bertness, Sarah R. Kurtz, and J. M. Olson, Phys. Rev. B **50**, 7509 (1994).
[30] H. D. Fuchs, C. H. Grein, R. I. Devlen, J. Kuhl, and M. Cardona, Phys. Rev. B **44**, 8633 (1991).